Supporting Information

Multifunctional and multi-site interfacial buffer layer for Efficient and stable perovskite solar cells

Pengyu Su[a, b, c], Huan Bi[d], Du Ran[a], Li Liu[e]*, Wenjing Hou[g], Guangzhao Wang[a, b, c], Wenbing Shi[f]**

[a]School of Electronic Information Engineering, Yangtze Normal University, No. 16, Juxian Avenue, Fuling District, Chongqing, P. R. China, 408100.

[b]Department of Applied Physics, Chongqing University, No. 174, Main Street, Shapingba District, Chongqing, P. R. China, 400044.

[c]Longxin Industry Co., Ltd, Chongqing, P. R. China, 400000.

[d]Graduate School of Informatics and Engineering, The University of Electro-Communications, 1-5-1 Chofugaoka, Chofu, Tokyo, Japan, 182-8585.

[e]Joint Laboratory for Extreme Conditions Matter Properties, School of Mathematics and Physics, Southwest University of Science and Technology, Mianyang, P. R. China, 621010.

[f]Chongqing Key Laboratory of Inorganic Special Functional Materials, College of Chemistry and Chemical Engineering, Yangtze Normal University, No. 16, Juxian Avenue, Fuling District, Chongqing, P. R. China, 408100.

[g]Institute of Molecular Science, Key Laboratory of Materials for Energy Conversion and Storage of Shanxi Province, Shanxi University, Taiyuan P. R. China, 030006.

Corresponding Authors

E-mail:hbi.trans.sci@uec.ac.jp (Huan Bi)

E-mail: liuli_phy@swust.edu.cn (Li Liu)

E-mail: swb@yznu.edu.cn (Wenbing Shi)

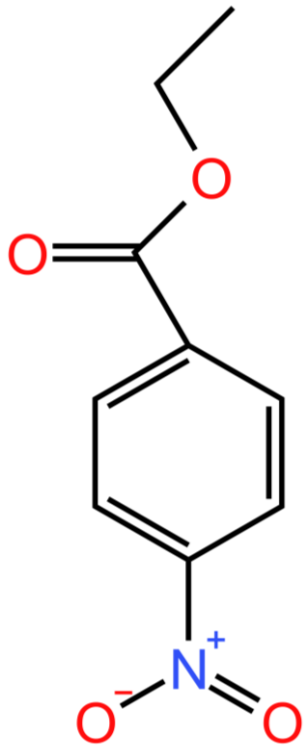

Fig. S1 Chemical structure used in this work.

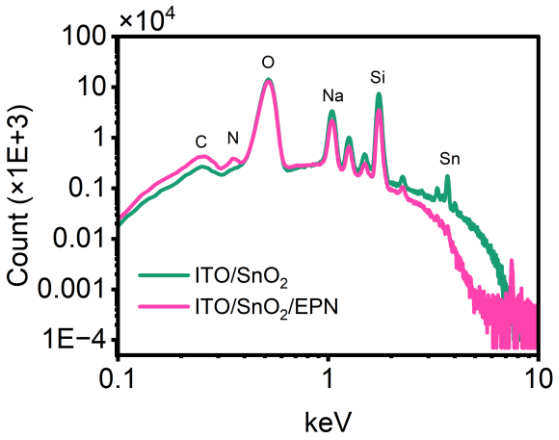

Fig. S2 EDS test of the sample with the structure ITO/SnO_2 and ITO/SnO_2/EPN.

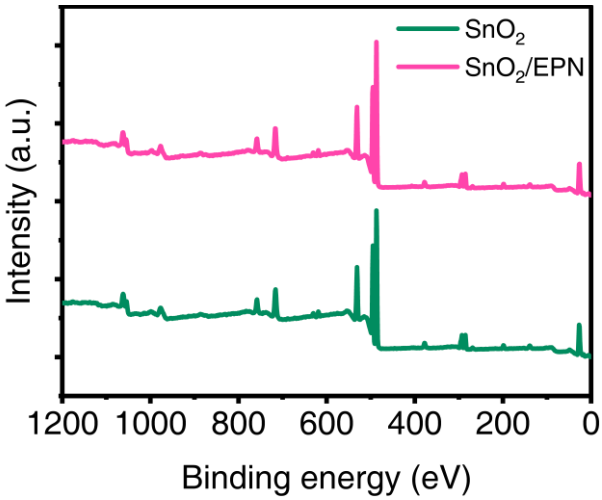

Fig. S3. Full XPS spectra of the SnO_2 and SnO_2/EPN films.

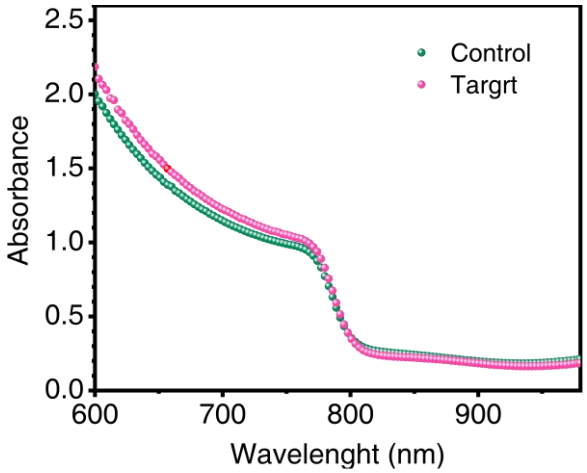

Fig. S4. UV-Vis absorption spectra of perovskite films deposited on SnO_2 (control) and SnO_2/EPN (target).

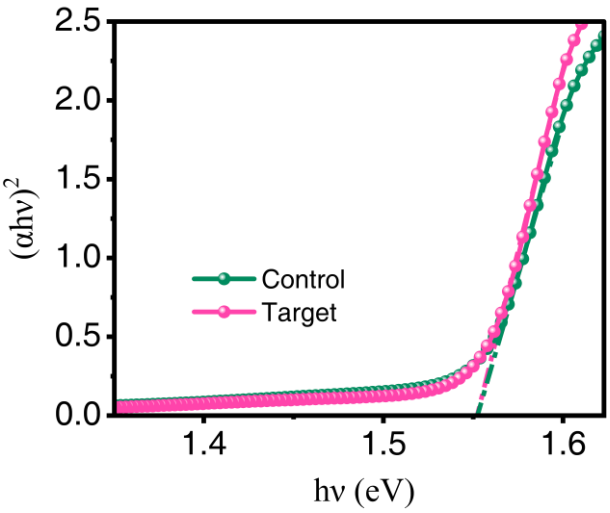

Fig. S5. Tauc plot of the control and target perovskite film obtain from the UV-vis data.

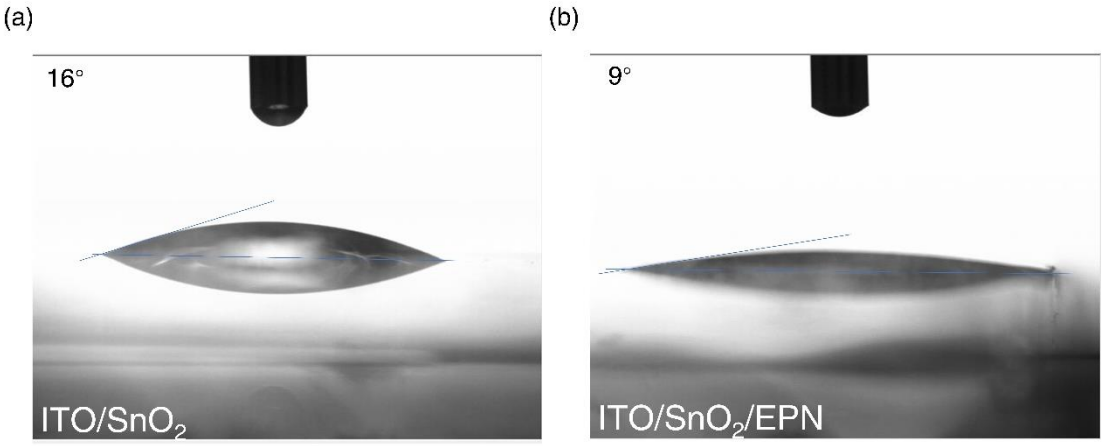

Fig. S6 Contact angle of the perovskite solution deposited on the (a) ITO/SnO_2 and (b) ITO/SnO_2/EPN.

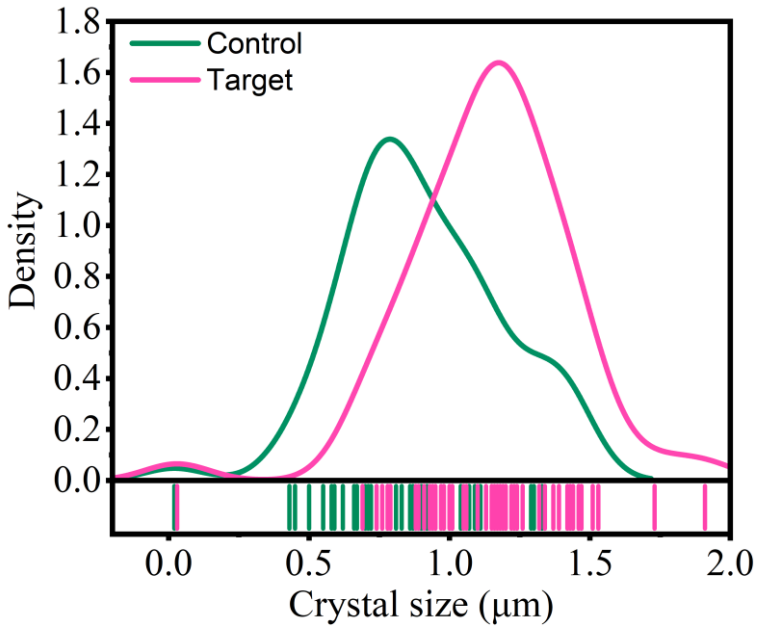

Fig. S7 Grain sizes statistics of the perovskite film deposited on SnO_2 with or without EPN modification.

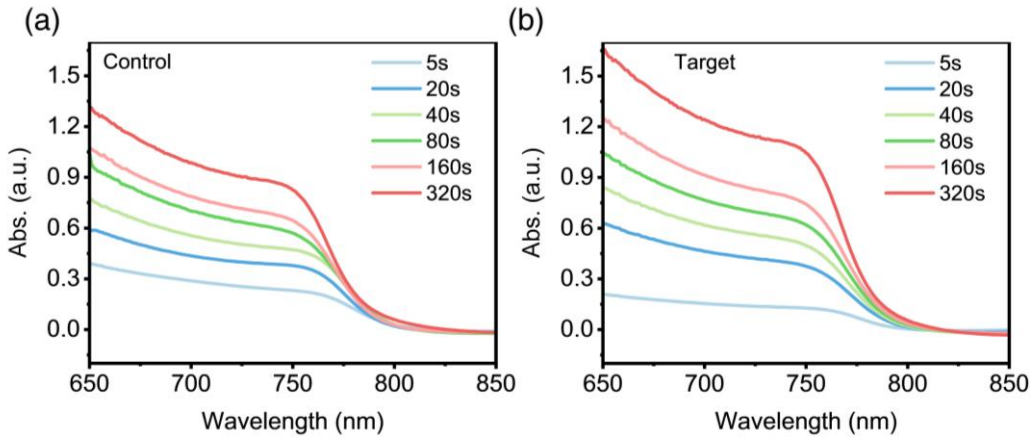

Fig. S8 UV–vis absorption spectra of the perovskite films c) without and d) with EPN annealed for different times.

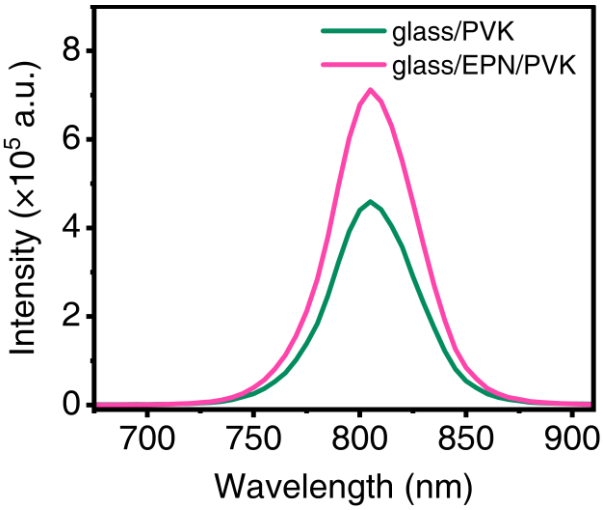

Fig. S9. PL curves of the perovskite film with the structure of glass/perovskite (treated with or without EPN).

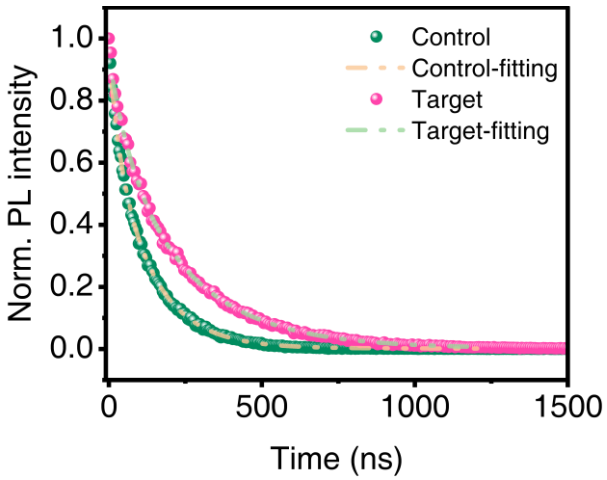

Fig. S10. TRPL curves of the perovskite film with the structure of glass/perovskite (treated with or without EPN).

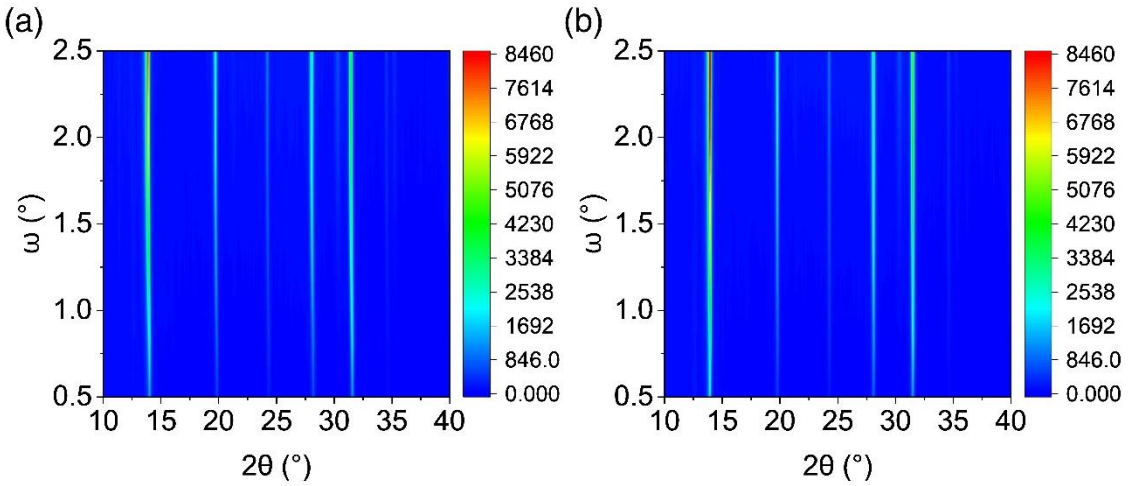

Fig. S11 Depth-dependent GIXRD patterns of the perovskite films with the structure of (a) ITO/SnO_2/perovskite and (b) ITO/SnO_2/EPN/perovskite.

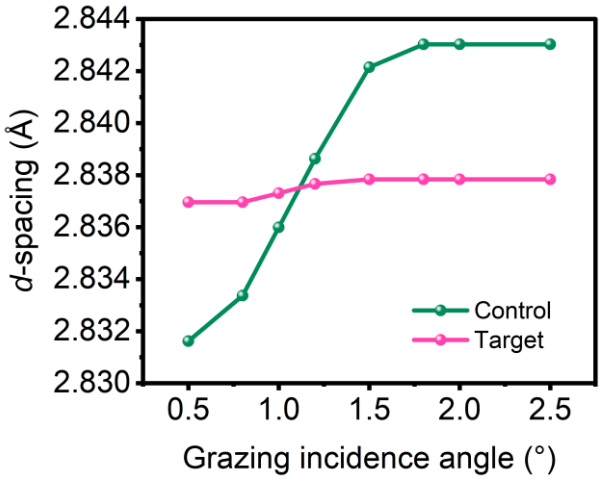

Fig. S12 *d*-spacing values obtained from {001} plane as a function of incidence angles.

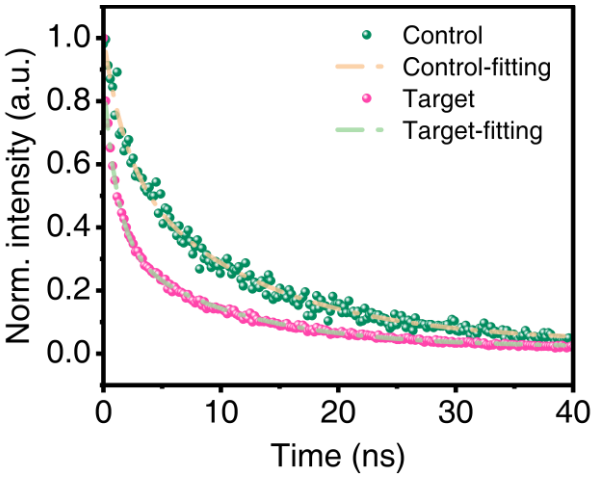

Fig. S13. TRPL curves of the perovskite film with the structure of ITO/SnO_2/perovskite (treated with or without EPN).

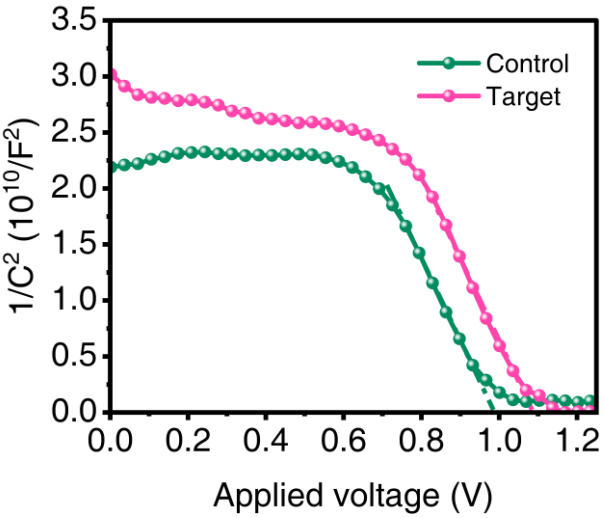

Fig. S14. Mott–Schottky analysis of SnO_2 and SnO_2/EPN based devices.

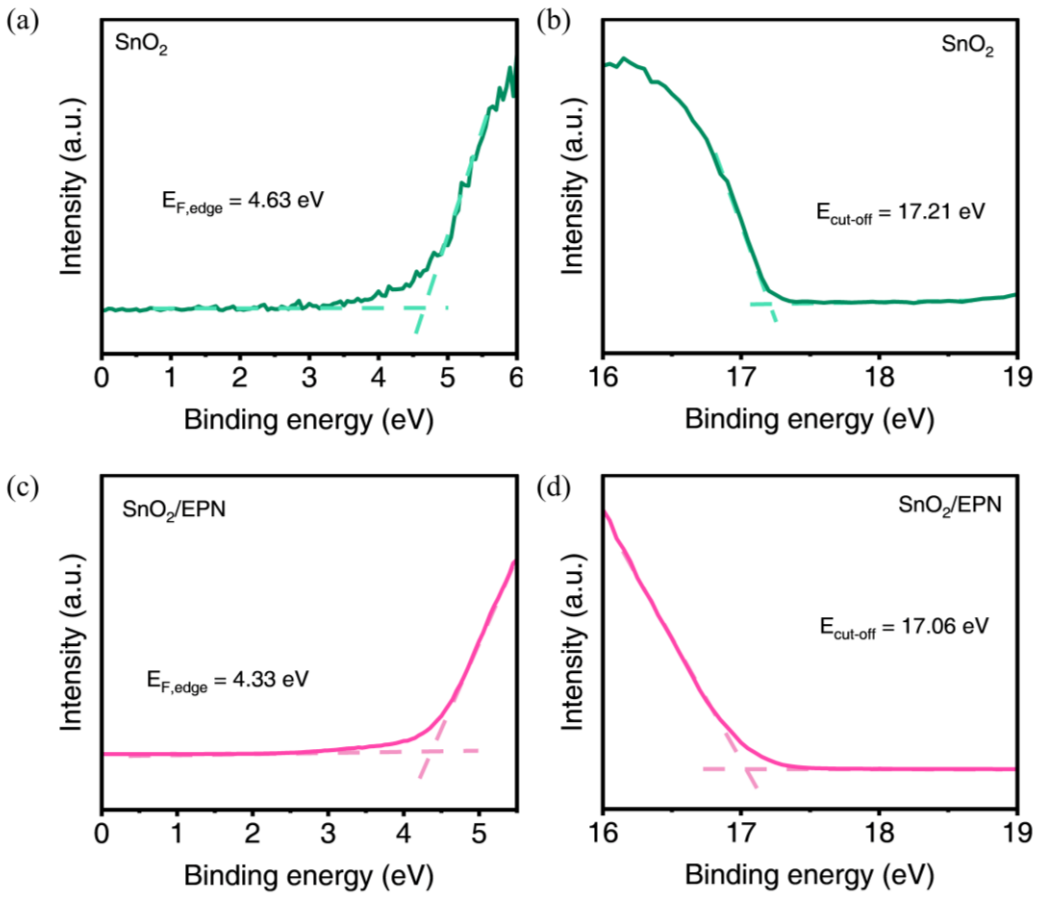

Fig. S15. UPS spectra of the unmodified SnO_2 and the EPN-modified SnO_2 (SnO_2/EPN) (a and c) the cut-off energy ($E_{cut\text{-}off}$) and (b and d) Fermi edge ($E_{F,\,edge}$).

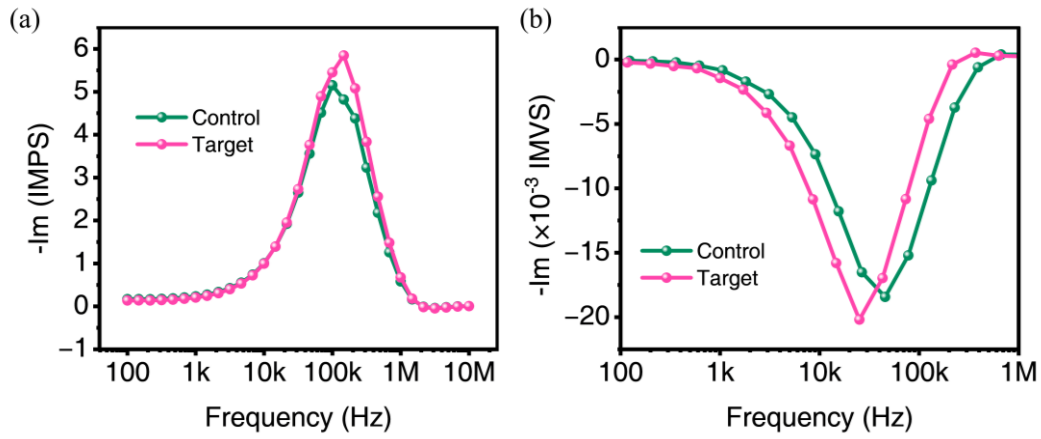

Fig. S16. (a) IMPS plot and (b) IMVS plot of PSCs with or without EPN modification.

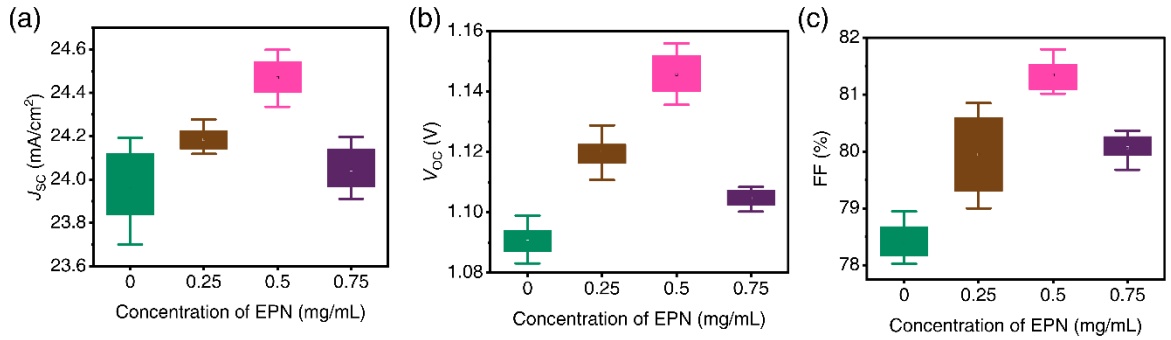

Fig. S17. Statistical photovoltaic parameters (J_{SC}, V_{OC} and FF) of solar cells at various concentrations of EPN.

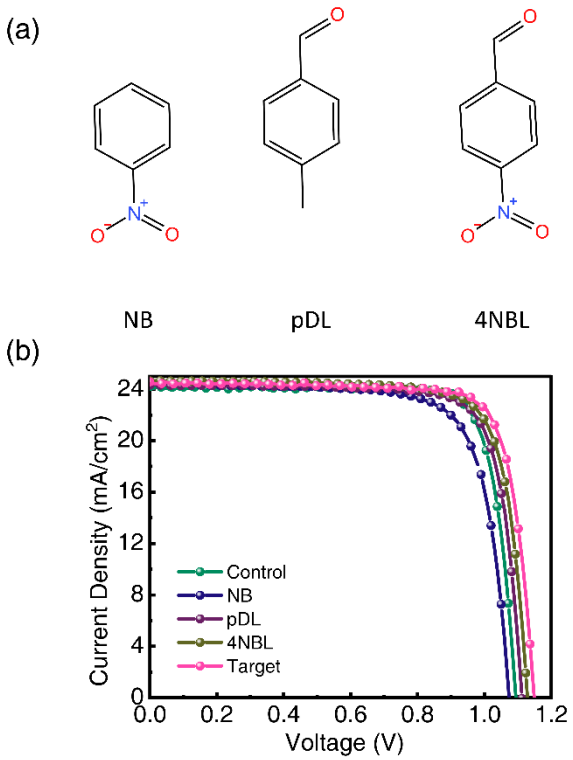

Fig. S18. (a) Chemical structures of the reference passivation molecules employed in this work. (b) *J-V* curves of the devices based on different modifiers. *J-V* curves were measured FS at a scan rate of 100 mV/s under simulated AM 1.5G one sun illumination of 100 mW/cm^2.

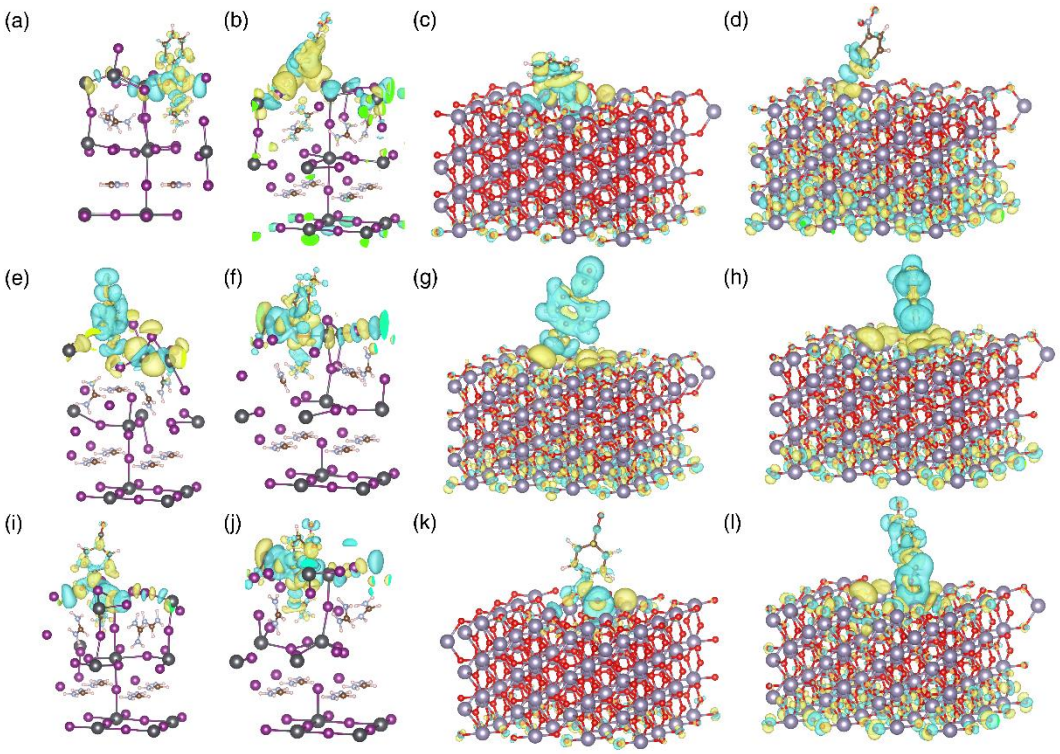

Fig. S19. The differential charge densities of (a) NB, (b) pDL and (c) 4NBL contact with SnO_2 and perovskite with different contact mode.

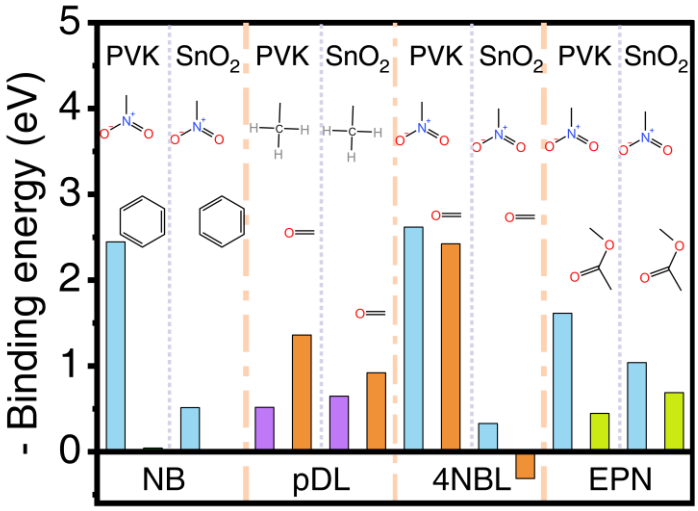

Fig. S20. Binding energy of NB, pDL, 4NBL and EPN contact with SnO_2 and perovskite with different contact mode.

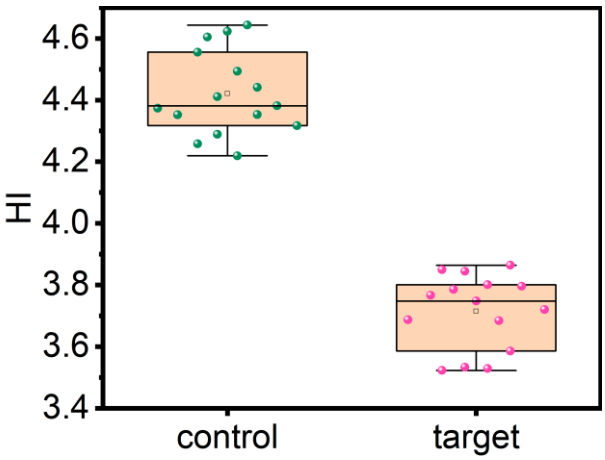

Fig. S21 Statistical hysteresis index (HI) distribution calculated from individual 15 cells.

Table S1. Fitted results of TRPL curves of the perovskite films deposited on glass or glass/EPN.

	Glass/PVSK	Glass/EPN/PVSK
τ_1 (ns)	32.511	68.436
%	0.234	0.241
τ_2 (ns)	129.850	243.453
%	0.729	0.704
τ_{ave} (ns)	122.529	228.096

Table S2. Fitted results of TRPL curves of the perovskite films deposited on ITO/SnO_2 or ITO/SnO_2/EPN.

	ITO/SnO_2	ITO/SnO_2/EPN
τ_1 (ns)	1.858	1.178
%	0.380	0.518
τ_2 (ns)	11.714	8.095
%	0.590	0.239
τ_{ave} (ns)	10.801	6.434

Table S3. The fitted EIS parameters of the devices based on SnO_2 and SnO_2/EPN ETLs.

ETL	R_s (Ω)	R_{rec} (kΩ)
SnO_2	8.93	31.4
SnO_2/EPN	8.41	41.8